Bioorganic & Medicinal Chemistry Letters 19 (2009) 1522–1527

Contents lists available at ScienceDirect

Bioorganic & Medicinal Chemistry Letters

journal homepage: www.elsevier.com/locate/bmcl

Synthesis and optimization of arylsulfonylpiperazines as a novel class of inhibitors of 11β-hydroxysteroid dehydrogenase type 1 (11β-HSD1)

Daqing Sun *, Zhulun Wang, Mario Cardozo, Rebekah Choi, Michael DeGraffenreid, Yongmei Di, Xiao He, Juan C. Jaen †, Marc Labelle ‡, Jinsong Liu, Ji Ma, Shichang Miao †, Athena Sudom, Liang Tang, Hua Tu, Stefania Ursu, Nigel Walker, Xuelei Yan, Qiuping Ye, Jay P. Powers †

Amgen Inc., 1120 Veterans Boulevard, South San Francisco, CA 94080, USA

ARTICLE INFO

Article history:
Received 18 October 2008
Revised 23 December 2008
Accepted 31 December 2008
Available online 9 January 2009

Keywords:
11β-HSD1
11β-HSD2
Diabetes
Metabolic syndrome
Hydroxysteroid dehydrogenase
Arylsulfonylpiperazines

ABSTRACT

The synthesis and SAR of a series of arylsulfonylpiperazine inhibitors of 11β-HSD1 are described. Optimization rapidly led to potent, selective, and orally bioavailable inhibitors demonstrating efficacy in a cynomolgus monkey ex vivo enzyme inhibition model.

11β-Hydroxysteroid dehydrogenase type 1 (11β-HSD1) is a key enzyme that acts as an NADPH-dependent reductase capable of converting inactive 11β glucocorticoids such as cortisone into their active form, (e.g., cortisol), in specific tissues, such as liver, adipose, and brain tissues. Therefore, 11β-HSD1 regulates tissue-specific glucocorticoid levels.[1–4] Conversely, 11β-hydroxysteroid dehydrogenase type 2 (11β-HSD2), a structurally related isoenzyme of 11β-HSD1, catalyzes the conversion of cortisol to cortisone utilizing NAD as a cofactor. 11β-HSD2 is expressed in cells that contain the mineralocorticoid receptor (MR) and protects the MR by converting cortisol to the inactive form, cortisone.[5] Selective inhibition of 11β-HSD1 may be a viable therapeutic strategy for the treatment of metabolic syndrome and has attracted significant attention from the pharmaceutical research community.[6–13]

We previously reported arylsulfonylpiperazines as potent inhibitors of 11β-HSD1 in in vitro assays.[14,15] Although compound **1** (Fig. 1) exhibited excellent in vitro inhibition of human and mouse 11β-HSD1, it had poor water solubility and oral bioavailability in rats. In this communication, we described our optimization efforts on structural modifications of **1** to improve the potency and pharmacokinetic (PK) profiles of this class of arylsulfonylpiperazine 11β-HSD1 inhibitors. These efforts led us to the discovery of potent, selective, and orally bioavailable inhibitors showing excellent efficacy in a cynomolgus monkey ex vivo enzyme inhibition model.

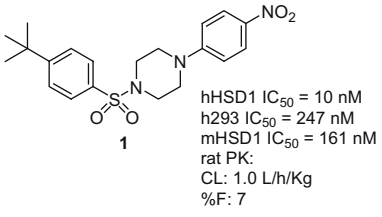

1

Figure 1. Arylsulfonylpiperazine 11β-HSD1 inhibitor.

Compounds were synthesized via the routes outlined in Schemes 1–5.[16] Compounds **2–8, 18–21**, and **30**, were prepared as shown in Scheme 1. Compounds **2–8** were obtained simply by reaction of *tert*-butylbenzenesulfonyl chloride and *N*-alkylpiperazine **31**, which was synthesized by either direct nucleophilic displacement between the alkyl halide and (*R*)-(−)-2-methylpiperazine or reductive amination of (*R*)-(−)-2-methylpiperazine with the appropriate aldehyde. Treatment of **31** with 4-acetylbenzenesulfonyl chloride in dichloromethane provided the

* Corresponding author. Tel.: +1 650 244 2195.
E-mail address: daqings@amgen.com (D. Sun).
† Present address: ChemoCentryx, Inc., Mountain View, CA 94043, USA.
‡ Present address: Lundbeck Research USA, Inc., 215 College Road, Paramus, NJ 07652, USA.

0960-894X/$ - see front matter © 2009 Elsevier Ltd. All rights reserved.
doi:10.1016/j.bmcl.2008.12.114

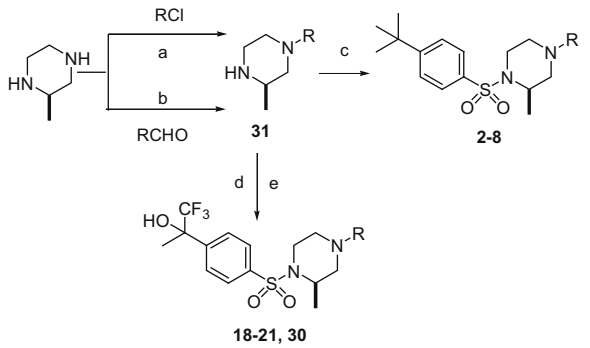

Scheme 1. Reagents and conditions: (a) MeCN, 100 °C, 45–75%; (b) $NaBH(OAc)_3$, acetic acid, CH_2Cl_2, 54–92%; (c) 4-*tert*-butylbenzenesulfonyl chloride, Et_3N, CH_2Cl_2, 65–84%; (d) 4-acetylbenzenesulfonyl chloride, Et_3N, CH_2Cl_2, 52–74%; (e) TMS-CF_3, TBAF, THF, 60–75%.

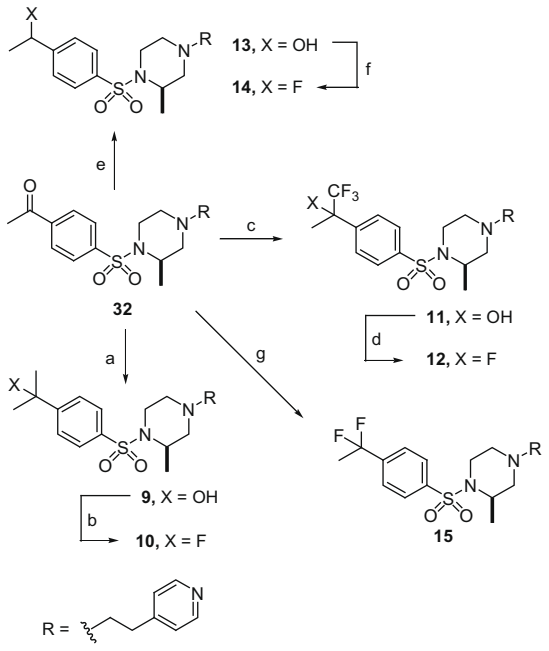

Scheme 2. Reagents and conditions: (a) MeLi, THF, 25%; (b) DAST, CH_2Cl_2, 21%; (c) TMS-CF_3, TBAF, THF, 63%; (d) DAST, CH_2Cl_2, 40%; (e) $NaBH_4$, MeOH, 92%; (f) DAST, CH_2Cl_2, 42%; (g) DAST, 25%.

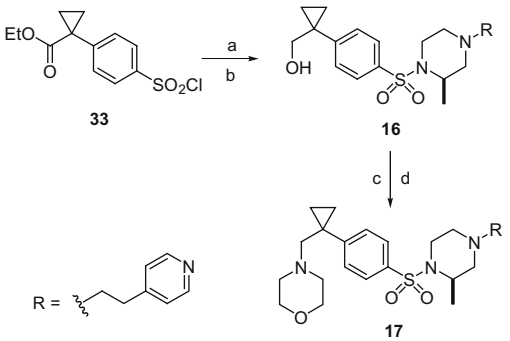

Scheme 3. Reagents and conditions: (a) **31**, Et_3N, CH_2Cl_2, 93%; (b) DIBAL-H, THF, 92%; (c) Dess–Martin periodinane, THF, 53%; (d) Morpholine, $NaBH(OAc)_3$, acetic acid, CH_2Cl_2, 27%.

corresponding ketone, which was converted to compounds **18–21, 30**, respectively, via treatment with TMS-CF_3. [17]

As shown in Scheme 2, compounds **9–15** were prepared from methyl ketone **32** using standard functional group transformations. Intermediate **32** was obtained by treatment of 4-acetylbenzenesulfonyl chloride with piperazine **31**, which was derived from direct nucleophilic displacement between 4-pyridylethyl chloride and (*R*)-(−)-2-methylpiperazine. Addition of methyl lithium to **32** formed alcohol **9**, which was subsequentially fluorinated with DAST in dichloromethane at −78 °C to afford **10**. Treatment with TMS-CF_3 converted **32** to trifluoromethylcarbinol **11**, which was fluorinated with DAST to afford **12**. Reduction of **32** with $NaBH_4$ provided **13**, which was converted to **14** with excess DAST at room temperature. In a similar fashion, compound **15** was prepared by treating **32** with DAST.

The synthetic route for preparing compounds **16–17** is shown in Scheme 3. Treatment of **31** with sulfonyl chloride **33** in dichloromethane gave the ester, which was then reduced with DIBAL-H to yield the alcohol **16**. Oxidation of the primary alcohol in **16**, followed by reductive amination of the resulting aldehyde with morpholine gave **17**.

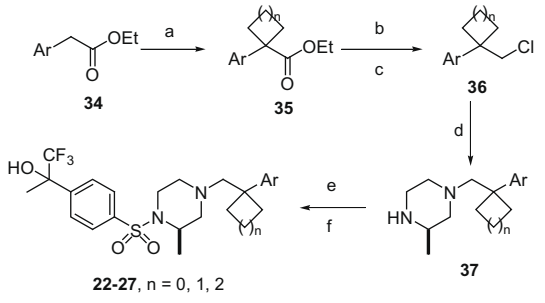

Scheme 4. Reagents and conditions: (a) NaH, $BrCH_2(CH_2)_nCH_2Br$, 49–80%; (b) DIBAL-H, THF, 49–54%; (c) $SOCl_2$, 83–84%; (d) (*R*)-(−)-2-methylpiperazine, MeCN, 100 °C, 75–83%; (e) 4-acetylbenzenesulfonyl chloride, Et_3N, CH_2Cl_2, 61–74%; (f) TMS-CF_3, TBAF, THF, 20–57%.

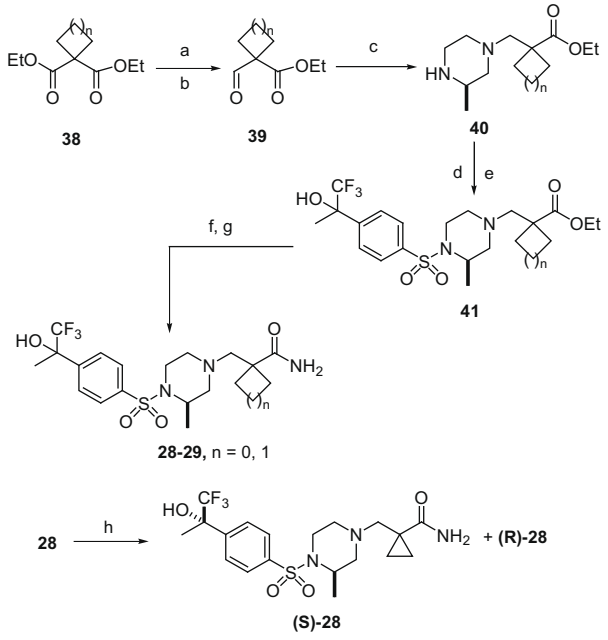

Scheme 5. Reagents and conditions: (a) $LiAl(O^tBu)_3H$, THF, 46%; (b) Dess–Martin periodinane, THF, 70%; (c) (*R*)-(−)-2-methylpiperazine, $NaBH(OAc)_3$, acetic acid, CH_2Cl_2, 80%; (d) 4-acetylbenzenesulfonyl chloride, Et_3N, CH_2Cl_2, 53%; (e) TMS-CF_3, THF, 78%; (f) LiOH, THF/MeOH/H_2O, 86%; (g) (i) $SOCl_2$; (ii) NH_3, 60%; (h) diastereoisomer separation.

The synthesis of compounds **22–27** is depicted in Scheme 4. Commercially available ester **34** was alkylated with appropriate dibromide to give **35**. Reduction of **35** with DIBAl-H, followed by chlorination of the primary alcohol with thionyl chloride produced chloride **36**, which was then coupled with (*R*)-(−)-2-methylpiperazine to yield **37**. Finally, preparations of compounds **22–27** were achieved by treatment of **37** with 4-acetylbenzenesulfonyl chloride, followed by trifluoromethylation with TMS-CF_3.

In Scheme 5, reduction of the appropriate ester **38** with lithium tri-*tert*-butoxyaluminohydride formed the corresponding alcohol, which was then oxidized to the aldehyde **39** with Dess–Martin periodinane. Reductive amination of **39** with (*R*)-(−)-2-methylpiperazine gave the substituted piperazine **40**, which was successively treated with 4-acetylbenzenesulfonyl chloride and trifluoromethylation with TMS-CF_3 to provide the ester **41**. Hydrolysis of **41** with lithium hydroxide gave the acid, which was treated with thionyl chloride and then ammonia to yield **28** or **29**, respectively. Separation of the diastereoisomers of **28** via preparative chiral HPLC (Chiralpak AD) afforded optically pure (*S*)-**28** and (*R*)-**28**.

Compounds were evaluated for the inhibition of human and mouse 11β-HSD1 enzymes, as well as in cell-based assays. 11β-HSD1 enzyme activity was determined by measuring the conversion of [^{3}H]-cortisone to [^{3}H]-cortisol. Product [^{3}H]-cortisol, captured by an anti-cortisol monoclonal antibody conjugated to scintillation proximity assay (SPA) beads, was quantified with a microscintillation plate reader. Biochemical enzyme assays were performed with Baculovirus-produced recombinant full-length human 11β-HSD1 as the enzyme source and NADPH as cofactor (h-HSD1 IC_{50}). Cell-based enzyme assays (h-293 IC_{50}) utilized HEK293 cells stably expressing recombinant human full-length 11β-HSD1 as the enzyme source without supplementation of NADPH. IC_{50} values for enzyme inhibition were calculated with a dose–response curve fitting algorithm with at least duplicate sets of samples.

Our initial optimization efforts began with the goal of improving the solubility of **1** by incorporating a carbon spacer between the aryl group and the piperazine ring. As shown in Table 1, the 4-pyridyl compounds (**3, 4, 5**, and **6**), which have a carbon based spacer, showed significant improvement in water solubility compared to **1** and **2**. Additionally, two or three-carbon spacers (**4** and **5**) and methyl substitution at the α-position of the 4-pyridyl group (**6**) resulted in potency similar to **2**. However, phenyl substitution at the α-position (**7**) notably reduced potency. The incorporation of an additional fused benzene ring (**8**) brought a slight decrease in potency as compared to **3**. These data suggested that both spacer length and substitution at the α-position were important for 11β-HSD1 inhibitory activity.

Based on metabolic liabilities we observed in our previous efforts,[14] i.e., in vitro oxidation of the *tert*-butyl group, we next turned our attention to modification of the substitution at the 4-position of the sulfonamide phenyl ring. Table 2 shows the effects of varying substituents at the 4-position of **4**. It was found that the trifluoromethylcarbinol moiety (**11**) produced approximately a threefold improvement in biochemical and cellular potency over the corresponding *tert*-butyl analog **4**, along with even more significant improvement in metabolic stability. No in vitro metabolite derived from the trifluoromethylcarbinol moiety was observed in metabolite identification studies.

With the discovery of the improved potency and metabolic stability imparted by the trifluoromethylcarbinol group as a substituent at the 4-position of the sulfonamide phenyl ring, we then returned to investigate further modifications of the *N*-alkyl substituents in **11**. The data in Table 3 indicated that 3-pyridyl derivative **18** was as potent as **11**, while the corresponding 2-pyridyl analog **19** exhibited decreased potency. Interestingly, the incorporation of fluorines to the α-position (**20, 21**) brought a slight increase of

Table 1
Inhibition of 11β-HSD1 by selected analogs: *N*-alkylation

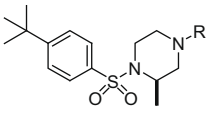

Compound	R	h-HSD1[a] IC_{50} (nM)	h-293[a] IC_{50} (nM)	Solubility (μg/mL) pH 5.0
2	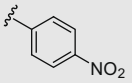	3	57	1.8
3	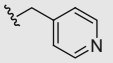	11.3	146	18.1
4	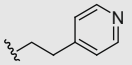	5.3	61	21.8
5	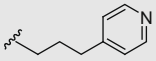	1	47	39
6	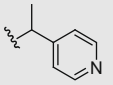	3.4	96	20.8
7	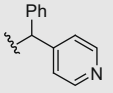	94	825	—
8	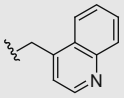	7.3	78	1.0

[a] Values are means of at least two determinations.

biochemical potency, but a decrease in cellular potency and in vitro metabolic stability as compared to **11** and **18**, respectively.

As *N*-dealkylation was observed as a significant metabolic liability in vitro, further investigation was carried out to introduce a cycloalkyl ring in the α-position of **11** and **18**. As indicated in Table 4, addition of a cycloalkyl ring gave a significant increase in biochemical potency with cyclopropyl, cyclobutyl, and cyclopentyl substituents (examples **22–27**, h-HSD1 IC_{50} < 1 nM), while cellular potency was mostly maintained relative to **11** and **18**. Furthermore, compound **22** also displayed significant improvement in in vitro metabolic stability over **11** (80% vs 59% remaining in rat liver S9 @ 60 min). The rat PK profile of **22** featured good oral bioavailability and a moderate clearance (F = 60%; CL = 2.1 L/h/kg). However, compound **22** also exhibited strong in vitro inhibitory activity against hERG and CYP-3A4 (Table 5).

In order to diminish the hERG and CYP-3A4 liability, alignment of pyridine analog **22** to a hERG pharmacophore model[18] was used to design modifications aimed at reducing hERG potency. Potent hERG blockers such as **22** aligned to the pharmacophore by matching two hydrophobic features and the ionizable nitrogen (Fig. 2) present in the inhibitors. This alignment suggested potential modifications to reduce the hERG liability. Replacement of the pyridine moiety, which matches one of the hydrophobic features, with polar groups were explored. Thus, compound **28** with an amide group replacing the pyridyl ring, was a much weaker hERG blocker than **22** (hERG IC_{50} **22**; 0.44 μM → **28**; >100 μM, Table 5). Additional modifications were made by adding hydrogen bond donor groups to the terminal aromatic ring targeting the so-called anti-hERG feature. Compound **30** with an amide at the *para*-position of phenyl ring, was a weak hERG blocker with an IC_{50} of 6.4 μM. Figure 2

Table 2
Inhibition of 11β-HSD1 by selected analogs: sulfonamide aryl modification

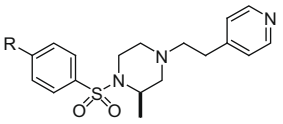

Compound	R	h-HSD1[a] IC_{50} (nM)	h-293[a] IC_{50} (nM)
4		5.3	61
9		5	69
10		36	—
11		2.2	21
12		4	71
13		12	70
14		16	138
15		30	86
16		4	55
17	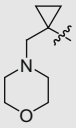	8	505

[a] Values are means of at least two determinations.

Table 3
In vitro inhibition and metabolic stability data for analogs **18–21**

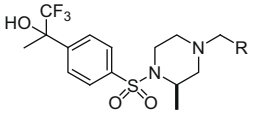

Compound	R	h-HSD1[a] IC_{50} (nM)	h-293[a] IC_{50} (nM)	Rat S9% remaining after 60 min
11	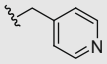	2.2	21	59
18	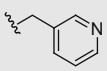	1.3	29	67
19	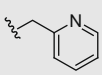	10	131	28
20	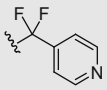	0.9	33	40
21	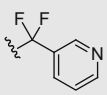	1.1	78	46

[a] Values are means of at least two determinations.

Table 4
In vitro inhibition and metabolic stability data for analogs **22–27**

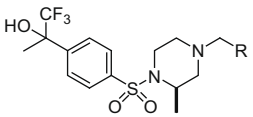

Compound	R	h-HSD1[a] IC_{50} (nM)	h-293[a] IC_{50} (nM)	Rat S9% remaining after 60 min
22	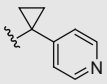	0.4	33	80
23	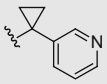	0.5	27	50
24	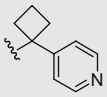	0.6	43	54
25	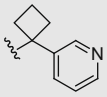	0.5	27	61
26	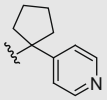	0.8	35	43
27	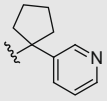	0.6	30	60

[a] Values are means of at least two determinations.

Table 5
CYP-3A4 and hERG inhibition potency of selected analogs

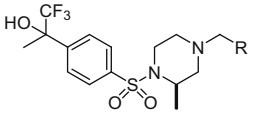

Compound	R	h-HSD1[a] IC_{50} (nM)	3A4 IC_{50} (μM)	hERG IC_{50} (μM)
2	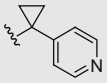	0.42	0.44	0.44
28	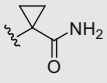	1.7	>100	>100
29	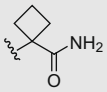	3.0	65	65
30	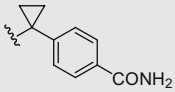	1.2	—	6.4

[a] Values are means of at least two determinations.

illustrates the alignment of compounds **22, 28**, and **30** against the hERG and anti-hERG pharmacophores.

Separation of the diastereoisomers of **28** was achieved by preparative chiral HPLC (Chiralpak AD) to afford the optically pure

(*S*)-**28**, a highly potent (hHSD1 IC_{50} = 0.7 nM) inhibitor of 11β-HSD1with excellent selectivity (hHSD2 IC_{50} > 100 μM) and no hERG and CYP liabilities (Table 6). Compound (*S*)-**28** also exhibited significant improvements in water solubility and oral bioavailability in rats compared to **1** (Table 7).

In addition to the excellent potency and pharmacokinetic profile of compound (*S*)-**28**, this molecule had suitable activity against cynomologous monkey 11β-HSD1 enzyme (IC_{50} = 6 nM) and was selected for further evaluation in our cynomolgus monkey ex vivo pharmacodynamic model. In this study, cynomolgus monkeys were dosed orally with 0.4, 2, and 10 mg/kg of inhibitor (*S*)-**28**. At 2 h post-dose, mesenteric fat tissues were collected. Following 1 h incubation of these tissues in media containing [^{3}H]-cortisone, 11β-HSD1 activity was measured through detection of tritiated cortisol levels using a scintillation proximity assay. Relative to controls, all dose groups showed a decrease in [^{3}H]-cortisol production in mesenteric fat (Fig. 3), corresponding to an ED_{50} in cynomolgus monkey of 0.4 mg/kg. These results demonstrate that (*S*)-**28** is effective in lowering 11β-HSD1 adipose activity in cynomolgus monkeys when administered orally. Compound exposure levels in this experiment were measured to be considerably higher in adipose than in plasma (Table 8), demonstrating that inhibitor (*S*)-**28** effectively distributed to the target tissue.

Finally, insight into the binding mode of this class of 11β-HSD1 inhibitors was obtained by X-ray crystallography (Fig. 4).[21] The co-

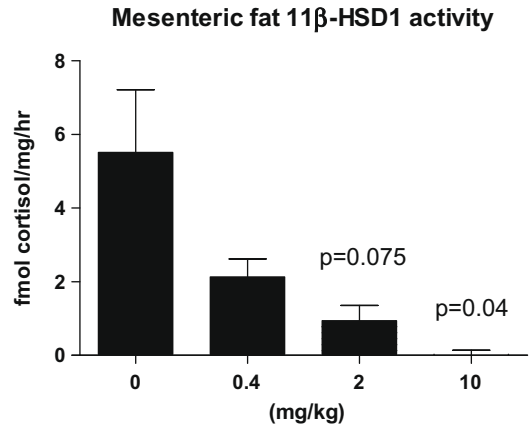

Figure 3. Ex vivo 11β-HSD1 enzyme activity in intact mesenteric fat collected from cynomolgus monkeys orally dosed with compound (*S*)-**28**. Plasma and mesenteric fat samples were collected 2 h after compound was administered orally in dosing vehicle (1% methylcellulose and 1% Tween 80 in sterile water). 11β-HSD1 enzyme activity was measured as the [^{3}H]-cortisol formed after 1 h incubation of fat samples in reaction buffer containing [^{3}H]-cortisone at 37 °C. Compound concentration in plasma and fat samples was determined with LC/MS/MS bio-analytic method.

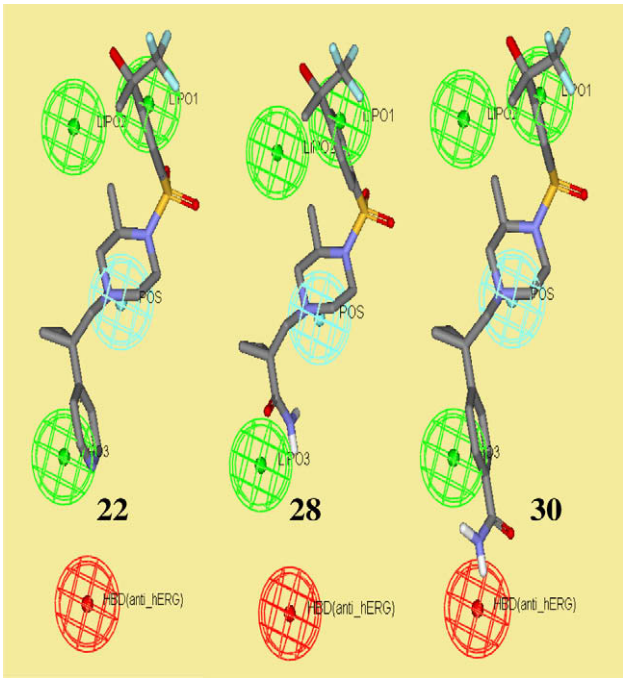

Figure 2. Alignment to hERG/anti-hERG pharmacophore.

Table 6
In vitro 11β-hSD1, CYP-3A4, and hERG inhibition potency of **28**, (*S*)-**28**, and (*R*)-**28**

Compound	h-HSD1[a] IC_{50} (nM)	h-293[a] IC_{50} (nM)	3A4 IC_{50} (μM)	hERG IC_{50} (μM)
28	1.7	25.4	>100	>100
(*S*)-**28**	0.7	14	>100	>100
(*R*)-**28**	7.9	128	>100	>100

[a] Values are means of at least two determinations.

Table 7
Solubility and rat PK data of **1** and (*S*)-**28**

Compound	AUC (po, μg h/L)	CL (iv, L/kg/h)	*F* (po, %)	Solubility (μg/mL) pH 5.0
1	29.8	1.0	7	0.5
(*S*)-**28**	638	1.4	41	>48.1

Dosed iv 0.5 mg/kg, po 2.0 mg/kg.

Table 8
Plasma and fat tissue exposure in cynomolgus monkeys after oral dosing with (*S*)-**28**

Po dose	*N*	[(*S*)-**28**] (μM) Plasma	[(*S*)-**28**] (μM) Mesenteric fat
Vehicle	4	BQL	BQL
0.4 mg/kg	3	0.029 ± 0.009	0.105 ± 0.036
2 mg/kg	3	0.349 ± 0.133	2.779 ± 1.537
10 mg/kg	3	0.503 ± 0.131	40.747 ± 20.874

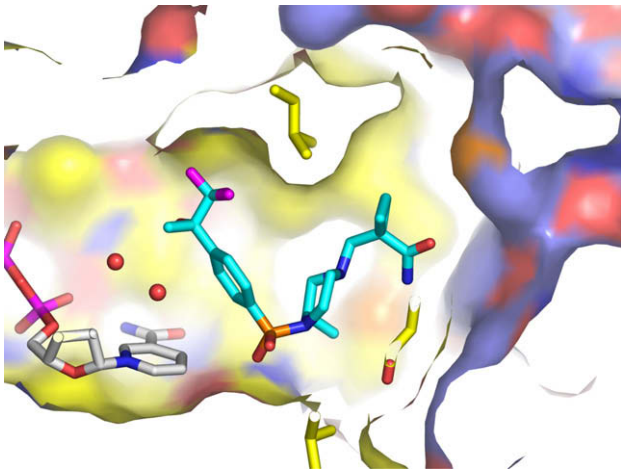

Figure 4. Co-crystal structure of compound (*S*)-**28** in human 11β-HSD1. The protein is shown in both stick and molecular surface representations which are color coded (red for oxygen atoms, blue for nitrogen, orange for sulfur, and slate for carbon). The inhibitor and the cofactor $NADP^+$ are shown in sticks and color coded gray for carbon atoms in $NADP^+$ and green for the inhibitor.

crystal structure of compound (*S*)-**28** with human 11β-HSD1 containing NADP cofactor reveals that the inhibitor binds to the substrate site in a V-shape with its trifluoromethylcarbinol group pointing towards the cofactor NADP+ side. The central sulfonyl group makes a hydrogen bond from one of its oxygen atoms to the backbone amide of Ala172, as well as VDW contacts with Ser170 in the catalytic site.

In summary, significant improvement in both potency and PK property was achieved by a series of modifications starting from **1**. Modification of the sulfonamide aryl substitution led to the discovery of the trifluoromethylcarbinol group, resulting in a threefold improvement in biochemical and cellular potency over the corresponding *tert*-butyl analog. Further modifications to the N-aryl substituents led to the discovery of a 1, 1-cyclopropyl spacer, producing a fourfold improvement in biochemical potency over the corresponding methylene compound. The hERG pharmacophore model was successfully used to reduce hERG potency. In addition, combination of the features resulted in a potent, selective, and orally bioavailable compound (*S*)-**28**, which demonstrated 11β-HSD1 inhibition in a cynomolgus monkey ex vivo model. Finally, X-ray co-crystallographic data of (*S*)-**28** with 11β-HSD1 revealed the key interactions for the inhibitor binding.

References and notes

1. Draper, N.; Stewart, P. M. *J. Endocrinol.* **2005**, *186*, 251.
2. Thieringer, R.; Hermanowski-Vosatka, A. *Expert Rev. Cardiovasc. Ther.* **2005**, *3*, 911.
3. Morton, N. M.; Paterson, J. M.; Masuzaki, H.; Holmes, M. C.; Staels, B.; Fievet, C.; Walker, B. R.; Flier, J. S.; Mullins, J. J.; Seckl, J. R. *Diabetes* **2004**, *53*, 931.
4. Tomlinson, J. W.; Walker, E. A.; Bujalska, I. J.; Draper, N.; Lavery, G. G.; Cooper, M. S.; Hewison, M.; Stewart, P. M. *Endocr. Rev.* **2004**, *25*, 831.
5. Seckl, J. S.; Walker, B. R. *Endocrinology* **2001**, *142*, 1371.
6. Barf, T.; Vallgarda, J.; Emond, R.; Haggstrom, C.; Kurz, G.; Nygren, A.; Larwood, V.; Mosialou, E.; Axelsson, K.; Olsson, R.; Engblom, L.; Edling, N.; Ronquist-Nii, Y.; Ohman, B.; Alberts, P.; Abrahmsen, L. *J. Med. Chem.* **2002**, *45*, 3813.
7. Hermanowski-Vosatka, A.; Balkovec, J. M.; Cheng, K.; Chen, H. Y.; Hernandez, M.; Koo, G. C.; Grand, C. B. L.; Li, Z.; Metzger, J. M.; Mundt, S. S.; Noonan, H.; Nunes, C. N.; Olson, S. H.; Pikounis, B.; Ren, N.; Robertson, N.; Schaeffer, J. M.; Shah, K.; Springer, M. S.; Strack, A. M.; Strowski, M.; Wu, K.; Wu, T.; Xiao, J.; Zhang, B. B.; Wright, S. D.; Thieringer, R. *J. Exp. Med.* **2005**, *202*, 517.
8. Olson, S.; Aster, S. D.; Brown, K.; Carbin, L.; Graham, D. W.; Hermanowski-Vosatka, A.; LeGrand, C. B.; Mundt, S. S.; Robbins, M. A.; Schaeffer, J. M.; Slossberg, L. H.; Szymonifka, M. J.; Thieringer, R.; Wright, S. D.; Balkovec, J. M. *Bioorg. Med. Chem. Lett.* **2005**, *15*, 4359.
9. Gu, X.; Dragovic, J.; Koo, G. C.; Koprak, S. L.; LeGrand, C. B.; Mundt, S. S.; Shah, K.; Springer, M. S.; Tan, E. Y.; Thieringer, R.; Hermanowski-Vosatka, A.; Zokian, H. J.; Balkovec, J. M.; Waddle, S. T. *Bioorg. Med. Chem. Lett.* **2005**, *15*, 5266.
10. Xiang, J.; Ipek, M.; Suri, V.; Massefski, W.; Pan, N.; Ge, Y.; Tam, M.; Xing, Y.; Tobin, J. F.; Xu, X.; Tam, S. *Bioorg. Med. Chem. Lett.* **2005**, *15*, 2865.
11. Coppola, G. M.; Kukkola, P. J.; Stanton, J. L.; Neubert, A. D.; Marcopulos, N.; Bilci, N. A.; Wang, H.; Tomaselli, H. C.; Tan, J.; Aicher, T. D.; Knorr, D. C.; Jeng, A. Y.; Dardik, B.; Chatelain, R. E. *J. Med. Chem.* **2005**, *48*, 6696.
12. (a) Yeh, V. S. C.; Patel, J. R.; Yong, H.; Kurukulasuriya, R.; Fung, S.; Monzon, K.; Chiou, W.; Wang, J.; Stolarik, D.; Imade, H.; Beno, D.; Brune, M.; Jacobson, P.; Sham, H.; Link, J. T. *Bioorg. Med. Chem. Lett.* **2006**, *16*, 5414; (b) Yeh, V. S. C.; Kurukulasuriya, R.; Madar, D.; Patel, J. R.; Fung, S.; Monzon, K.; Chiou, W.; Wang, J.; Jacobson, P.; Sham, H. L.; Link, J. T. *Bioorg. Med. Chem. Lett.* **2006**, *16*, 5408; (c) Yeh, V. S. C.; Kurukulasuriya, R.; Fung, S.; Monzon, K.; Chiou, W.; Wang, J.; Stolarik, D.; Imade, H.; Shapiro, R.; Knourek-Segel, V.; Bush, E.; Wilcox, D.; Nguyen, P. T.; Brune, M.; Jacobson, P.; Link, J. T. *Bioorg. Med. Chem. Lett.* **2006**, *16*, 5555; (d) St Jean, D. J., Jr.; Yuan, C.; Bercot, E. A.; Cupples, R.; Chen, M.; Fretland, J.; Hale, C.; Hungate, R. W.; Komorowski, R.; Veniant, M.; Wang, M.; Zhang, X.; Fotsch, C. *J. Med. Chem.* **2007**, *50*, 429.
13. Julian, L. D.; Wang, Z.; Bostick, T.; Caille, S.; Choi, R.; DeGraffenreid, M.; Di, Y.; He, X.; Hungate, R. W.; Jaen, J. C.; Liu, J.; Monshouwer, M.; McMinn, D.; Rew, Y.; Sudom, A.; Sun, D.; Tu, H.; Ursu, S.; Walker, N.; Yan, X.; Ye, Q.; Powers, J. P. *J. Med. Chem.* **2008**, *51*, 3953.
14. Sun, D.; Wang, Z.; Di, Y.; Jaen, J. C.; Labelle, M.; Ma, J.; Miao, S.; Sudom, A.; Tang, L.; Tomooka, C. S.; Tu, H.; Ursu, S.; Walker, N.; Yan, X.; Ye, Q.; Powers, J. P. *Bioorg. Med. Chem. Lett.* **2008**, *18*, 3513.
15. Tu, H.; Powers, J. P.; Liu, J.; Ursu, S.; Sudom, A.; Yan, X.; Xu, H.; Meininger, D.; DeDraffenreid, M.; He, X.; Jaen, J. C.; Sun, D.; Labelle, M.; Yamamoto, H.; Shan, B.; Walker, N.; Wang, Z. *Bioorg. Med. Chem.* **2008**, *16*, 8922.
16. All compounds gave satisfactory ^{1}H NMR, HPLC, and MS data in full agreement with their proposed structures and purity (>95%) was determined by HPLC analysis.
17. Prakash, K. G. S.; Yudin, A. K. *Chem. Rev.* **1997**, *97*, 757.
18. *hERG modeling method:* A Unity hERG pharmacophore, developed from literature data,[19] was used to align this analog series. The model consists of three hydrophobic (aliphatic as well as aromatic) groups and ionizable nitrogen. This pharmacophore is similar to that published by Cavalli et al.[20] In addition, we developed an anti-hERG feature consisted of a hydrogen bond donor of specific location relative to the hERG 'favorable' features. The location of the anti-hERG feature was derived from automatic molecular alignment of an internal hERG dataset. In this data, potent hERG blockers where modified with various types of hydrogen bond donors resulting in significant reduction of hERG binding and patch clamp IC_{50}. A Unity hydrogen bond donor feature was build based on this alignment and combined with the hERG pharmacophore.
19. Sybyl, version 7.0; Tripos, Inc.: St. Louis, MO, 2003.
20. Cavalli, A.; Poluzzi, E.; De Ponti, F.; Recanatini, M. *J. Med. Chem.* **2002**, *45*, 3844.
21. The atomic coordinate has been deposited in the Protein Data Bank under an accession code 3D4N.